Biosensors and Bioelectronics 126 (2019) 1–6

Contents lists available at ScienceDirect

Biosensors and Bioelectronics

journal homepage: www.elsevier.com/locate/bios

Facile and highly sensitive photoelectrochemical biosensing platform based on hierarchical architectured polydopamine/tungsten oxide nanocomposite film

Yanyan Yu[a,b,1], Zhongnan Huang[a,1], Yao Zhou[b], Lihua Zhang[a], Ailin Liu[a], Wei Chen[a,*], Jianhua Lin[c,*], Huaping Peng[a,*]

[a] School of Pharmacy, Fujian Medical University, Fuzhou 350004, Fujian Province, China
[b] School of Pharmacy, Nantong University, Nantong 226001, Jiangsu Province, China
[c] Fujian Platform for Medical Research at First Affiliated Hospital, Fujian Key Lab of Individualized Active Immunotherapy, Fuzhou 350005, Fujian Province, China

ARTICLE INFO

Keywords:
Tungsten oxide
Photoelectrochemistry
Polydopamine
Biosensor
CYFRA 21-1

ABSTRACT

The fabrication of photosensitive interface and molecular recognition layer at the biosensing surface are of vital importance in photoelectrochemical (PEC) biosensor construction. Developing facial methods with favorable biomolecule immobilization as well as excellent photoelectric activity still need to be explored. In this work, by integration of the merits of tungsten oxide (WO_3) semiconductor nanomaterial and polydopamine (PDA) polymer, a novel biofunctional PDA/WO_3 nanocomposites (PDA/WO_3 NCs) modified ITO hierarchical architecture was fabricated by simple thermal annealing and self-polymerization methods. The proposed PEC biosensor platform based on PDA/WO_3/ITO not only have preponderances in simple preparation, but also possesses excellent PEC activity, high specific surface area and good microenvironment for biomolecule immobilization. Utilizing CYFRA 21-1 as a model target, label-free PEC immunosensor was developed successfully, which exhibited great sensitivity and broad dynamic range with four orders of magnitude (10 pg mL^{-1} to 100 ng mL^{-1}), and the limit of detection was as low as 2.5 pg mL^{-1}. Moreover, owing to the great sensitivity and selectivity of the proposed platform, this convenient sensor also performed well in real serum sample analysis. It is worth noting that our work not only helps in gaining a better understanding of the applicability of the PEC properties of PDA/WO_3 NCs, but also sheds novel light on the design and development of PEC biosensing platform based on PDA/WO_3 NCs.

1. Introduction

Photoelectrochemical (PEC) biosensors are widely regarded as an innovative and powerful method for bioanalysis, due to the inherent sensitivity and the specific bioaffinity properties of the biomolecules. Up to now, PEC technique has been applied to determine various targets, ranging from small molecules to large proteins (Zhang et al., 2017; Zhao et al., 2018). The choice of photoelectric active material is of great concern to achieve excellent PEC performance. Organic photoelectric active material, conductive macromolecule and inorganic semiconductor and their composite materials are all widely used to fabricate the photoelectric conversion unit (Zang et al., 2017; Zhao et al., 2015, 2017). Various semiconductor materials are one of the extensively explored materials for PEC biosensors construction. Particularly, tungsten oxide (WO_3), an n-type semiconductor material, with a band gap of 2.5–2.8 eV, has aroused great interest due to the merits of excellent carrier mobility, chemical stability and thermostability (Peng et al., 2017, 2016; Wang et al., 2017a; Yang et al., 2018). Whereas, the intrinsic photoelectric activity of WO_3 was not satisfactory due to its narrowband gap and high electric-hole recombine rate. By coupling CdS or other semiconductors with WO_3 nanomaterials to form a heterojunction structures (eg. WO_3/TiO_2, WO_3/g-C_3N_4, WO_3/Sb_2S_3, $WO_3/AgIO_3$) is a common way to facilitate the electron-hole pairs apart and thus reduce the chance of recombination (Han et al., 2018; Tan et al., 2018; Wang et al., 2016; Zhang et al., 2016). However, the heterostructures are always hard to prepare and not environmental friendly. Notably, the WO_3 interface is hard to immobilize biomolecules, thus hindering its application in PEC biosensors, as the biomolecule immobilization is crucial for the PEC biosensor performance. To improve the immobilization property of the WO_3 interface, Wu group prepared

* Corresponding authors.
E-mail addresses: weichen@fjmu.edu.cn (W. Chen), jianhual@fjmu.edu.cn (J. Lin), penghuaping@fjmu.edu.cn (H. Peng).
[1] These authors contributed equally to this work.

https://doi.org/10.1016/j.bios.2018.10.026
Received 16 July 2018; Received in revised form 27 September 2018; Accepted 13 October 2018
Available online 21 October 2018

AuNPs-functionalized WO_3 (WO_3-Au) hybrids for antibody immobilization through Au-NH_2 bonding (Wang et al., 2017b). But the procedures are sophisticated and requiring more than 16 h to incorporate the AuNPs onto the WO_3 interface. Therefore, it is essential to probe facial methods that can not only facilitate biomolecule immobilization, but also improve the photoelectric activity and biocompatibility at the same time.

Indeed, surfaces engineering is crucial in fabrication of biosensors or biodevices. The biosensing interface is supposed to be biocompatible. Generally speaking, the general methods for the interface fabrication, including chemical hydrolysis, layer assembly, and plasma treatment, are inevitably time-consuming and laborious. Mostly, they are surface specific (Kumar and Rao, 2015; Whaley et al., 2000). Therefore, developing a facial method is still challenging and urgent. The research about the invertebrate mussel adhesion inspired great advance in the surface modification. Enlightened by these findings, polydopamine (PDA) was firstly reported as a fascinating coating material (Lee et al., 2007) because of its similar molecular structure to 3,4-dihydroxy-L-phenylalanine (DOPA), which is the key molecule for the powerful adhesion of mussels. In the presence of oxygen, dopamine can self-polymerize into PDA, which can be employed to deposit on almost all kinds of substrates (Cai et al., 2017; Qu et al., 2017). Due to the presence of reactive groups, PDA film offers further biomolecule immobilization for biosensors and biochips construction. And various biosensing interfaces, including glucose oxidase, sulfate-reducing bacteria, interleukin-6 and human immunoglobulin G, have all been developed through facial cross linking. Combining with nanoparticles, PDA can also form signal amplification platforms for biomolecules. (Liu et al., 2014). Interestingly, PDA film also possesses intriguing optical properties and also has been explored recently as a sensitizer to improve the PEC performance of semiconductors by shortening the carrier diffusion distance, improving light harvesting efficiency and charge collection efficiency (Dong et al., 2017; Ryu et al., 2015; Wei et al., 2013).

Non-small cell lung cancer (NSCLC) accounts for approximately 80% lung cancer cases. The 5-year survival rate of NSCLC is less than 50–70% owing to the high morbidity and poor prognosis (Soria et al., 2017). Thus, it is vital for patients to be diagnosed early and treated positively to improve the prognosis and survival rate. Up to now, a number of biomarkers have been discovered to diagnose NSCLC. Among them, CYFRA 21-1 (Grunnet and Sorensen, 2012), a soluble cytokeratin 19 (CK19) fragment, has been reported to be the most valuable biomarker of NSCLC treatment. In the past decades, various strategies have been developed for CYFRA 21-1 determination, including backscattering interferometry (Olmsted et al., 2014), field-effect transistor arrays (Lu et al., 2015), multiplexed near-infrared (NIR) method (Liu et al., 2016), electrochemical (Kumar et al., 2018) and fluorescence (Chen et al., 2017) immunoassay etc. But the poor sensitivity and labeling steps, to some extent, have hindered their widespread application. Thus, facial detection method with high sensitivity remains to be explored.

Herein, by integration of the merits of WO_3 nanomaterial and PDA, a novel PEC immunosensor using bioinspired PDA functionalized WO_3 nanocomposites (PDA/WO_3 NCs) modified ITO electrode has been developed. As shown in Scheme 1, the WO_3 was prepared by annealing of tungsten disulfide nanoparticles (WS_2 NPs) modified electrode, and the PDA was coated by spontaneously self-polymerization of dopamine. The as-prepared WO_3 modified ITO electrode showed good PEC activity, and the yielding anodic photocurrent could be obviously enhanced by coating of PDA film. Furthermore, the PDA coating could provide a compatible interface for antibody (Ab) immobilization. Taken CYFRA 21-1 as an example, due to the formation of the immunocomplex, the concentrations of CYFRA 21-1 were determined through the decrease in photocurrent intensity. By integration of the excellent biocompatibility and biomolecular immobilization property of the PDA/WO_3 NCs, the proposed PEC sensor offered an efficient platform for reliable PEC immunoassay. And the platform also exhibited great potential for application to other biomolecules assay, such as cells, DNA and proteins.

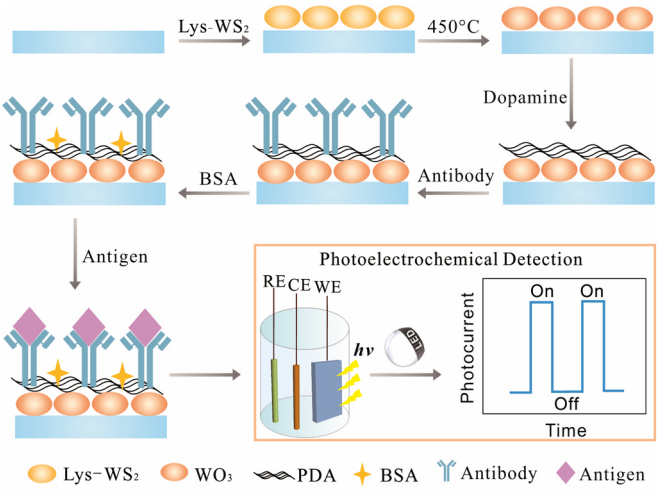

Scheme 1. Schematic illustration of the PDA/WO_3/ITO PEC immunosensor.

2. Experimental section

2.1. Reagents and apparatus

WS_2 (90 nm), ascorbic acid and dopamine were from Sigma—Aldrich (Shanghai, China). L-cysteine (Lys), potassium ferricyanide, potassium ferrocyanide, Tris(hydroxymethyl) aminomethane (Tris), Na_2HPO_4 and NaH_2PO_4 were obtained from Sinopharm Chemical Reagent Company (Shanghai, China). Bovine serum albumin (BSA) was obtained from Shanghai Sangon Biological Engineering Technology and Services Co., Ltd. (China). CYFRA21-1antigen (CYFRA21-1Ag) and CYFRA21-1 antibody (CYFRA21-1Ab), carcino-embryonic antigen (CEA) and fibronectin (FN) were from InnoDx Biotechnology Co., Ltd. (Xiamen, China). ELISA kit was purchased from Boster Biological Technology Co. Ltd. (Wuhan, China). All chemical reagents were directly used without further purification. Ultrapure water (18.2 MΩ/cm) from Millipore Milli-Q system was utilized throughout the experiment.

Photoelectrochemical measurements were conducted with a home-built photoelectrochemical system with a 5 W LED lamp as the irradiation source. All PEC measurements were performed with an electrochemical analyzer (CHI760D, Chenhua Co., Shanghai, China). A three-electrode system: an ITO modified electrode as the working electrode (WE), an Ag/AgCl (saturated KCl solution) electrode as the reference electrode (RE), and a Pt wire as the counter electrode (CE) was employed all through the experiments. Energy dispersive spectrometer (EDS) and scanning electron microscope (SEM) images were obtained with JEM-2100 SEM instrument (JEOL, Japan). The Brunauer-Emmett-Teller (BET) surface area of the WO_3 samples were determined by physical adsorption-desorption of N_2 using Quantachrome AUTOSORB-1-C instrument (Tristar II 3020M).

2.2. Preparation of PDA/WO_3 modified ITO electrode

WO_3/ITO was prepared by facile annealing of WS_2/ITO. Firstly, the mixture of WS_2 (75 mg) and Lys (20 mL 1.25 mg mL^{-1}) was sonicated for 3 h. Then, the dispersion was centrifugated at 3000 rpm for 5 min to remove large-size masses,and the supernatant was collected by centrifugation at 10,000 rpm for 10 min. Then the soluble WS_2 nanoparticles were obtained after dispersion in water (5 mg mL^{-1}). The efficient surface areas of ITO electrodes (ϕ = 4 mm) were fixed with polydimethylsiloxane (PDMS). Before modification, the ITO electrode surface was cleaned by sonicating in 1 M NaOH, 30% H_2O_2, cetone for 5 min in turn. The electrode was dried with nitrogen stream prior to further use. Then the prepared Lys-WS_2 nanocomposite (40 μL) was dropped onto the surface of the ITO and dried at room temperature

before the electrode was annealed at 450 °C for 30 min. In this process, the WS_2 was oxidized to WO_3, thus, WO_3/ITO electrode was modified.

The PDA/WO_3/ITO electrode was prepared as follows: to grow PDA thin film on WO_3, the WO_3/ITO electrode was immersed in 1 mL dopamine solution (5 mg mL^{-1}, pH 8.5) at 4 °C for 2 h. Owing to the self-polymerization process, the PDA coated WO_3/ITO electrode (PDA-WO_3/ITO) was obtained.

2.3. PEC immunosensor construction

Firstly, 15 μL of 0.2 mg mL^{-1} CYFRA21-1Ab was dropped onto the electrode surface. After incubating overnight at 4 °C, the electrode was washed with water. Then, 50 μL BSA (1%) was dropped and the electrode was incubated for 1 h before rinsed.

The performance of the immunosensor was investigated by analyzing the concentration of CYFRA21-1. Briefly, different concentrations of CYFRA21-1(15 μL) were incubated with the PDA-WO_3/ITO electrode for 60 min at 37 °C (Fig. S1). After being washed with water, the electrode was immersed into 0.1 M phosphate buffered saline (PBS, pH 7.4) containing 5 mM AA for PEC detection.

3. Results and discussion

3.1. Characterization of the nanomaterials

The microstructure and morphology of the synthesized nanomaterials were characterized by SEM. Fig. 1A demonstrated that the water-soluble Lys-WS_2 nanocomposite presented agglomerated nanoparticles morphology. After thermal annealing, the hierarchical architecture still remained (Fig. 1B). The EDS spectra shown in Fig. 1D confirmed that the Lys-WS_2 nanocomposite mainly contained W, S as well as little C, N, O elements, due to the presence of Lys. In comparison, there was not any S found in the samples after annealing, while O element content increased prominently, indicating that WS_2 was oxidized to WO_3 (Mandal et al., 2018). Brunauer-Emmett-Teller (BET) measurements revealed that WO_3 nanomaterial possessed the specific surface area of 6.2 m^2 g^{-1}. While the geometric area of the electrode was 0.1256 cm^2, which was much smaller than the area of WO_3 nanomaterial modified electrode (estimated to be 12.4 cm^2). These results indicated that the prepared WO_3 nanomaterial could effectively increase the specific surface area of the modified electrode. It has been reported that the dopamine monomer can be oxidized and spontaneously self-polymerize under alkaline conditions (pH > 7.5) with oxygen as the oxidant. The oxidation process leads to the formation of dopaminequinone which rapidly undergoes cyclisation through a Michael type cycloaddition (Ball, 2018). This polymerization reaction is mild without any complicated instrumentation or harsh reaction conditions. Due to the versatility and ease of secondary functionalization, enormous research effort has been devoted to applications of PDA films (Lee et al., 2007; Liu et al., 2014). In this work, the PDA polymerization was conducted at 4 °C in order to obtain a thin film on the surface of the WO_3 nanomaterial by reduce reaction kinetics in low temperature. As shown in Fig. 1C, the morphology of the PDA-WO_3 nanomaterial modified electrode remained the same agglomerated nanoparticles morphology with WO_3, which would also effectively increase the specific surface area of the modified electrode. The resulting PDA-WO_3 nanomaterial yielded an even higher oxygen content than WO_3 (Wei et al., 2013). Hence, the final composites with large specific surface area and functional groups could act as perfect scaffold to assemble biomolecules, which was beneficial for PEC assay.

3.2. Characterization of the PEC immunosensor

Firstly, the stepwise modification process of the immunosensor was investigated with electrochemical impedance spectroscopy (EIS) to characterize the interface behaviors of electrodes (Fig. 1E). After modification with WO_3, the ITO electrode exhibited a relatively small

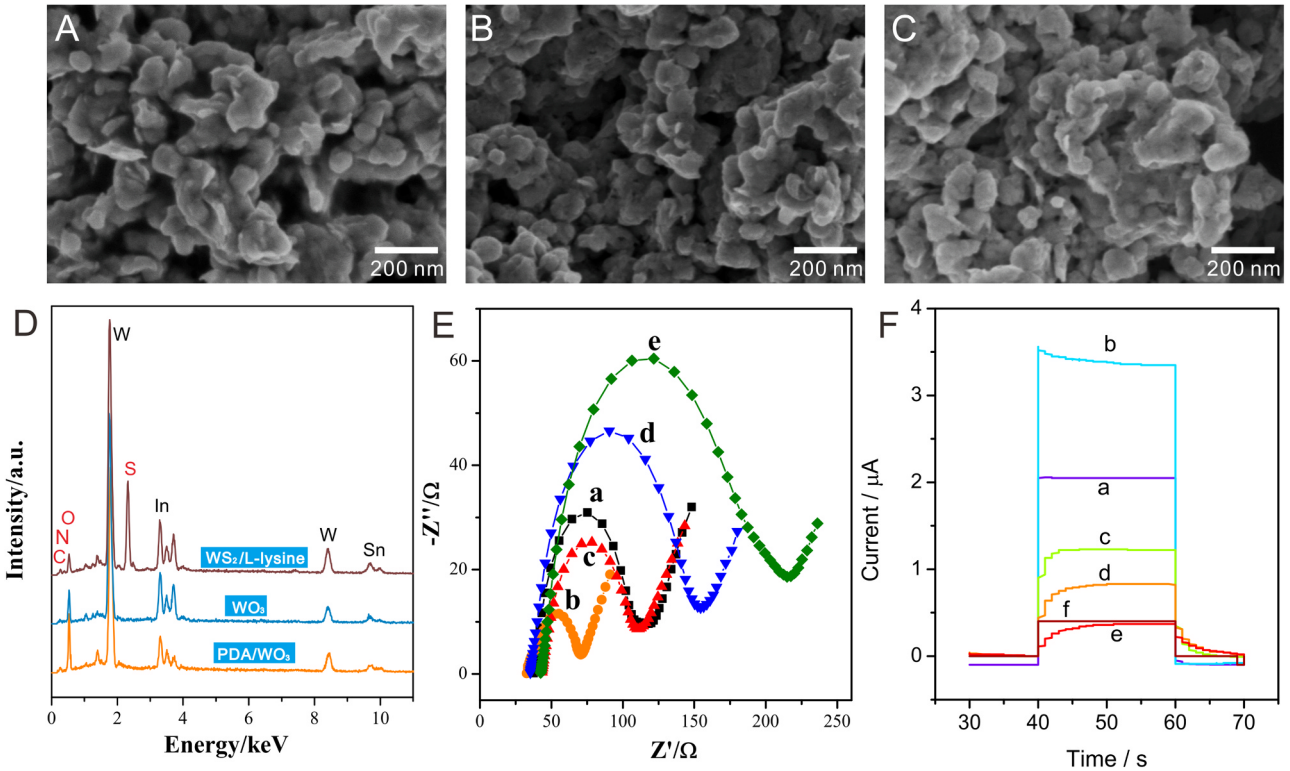

Fig. 1. The SEM images of (A) Lys-WS_2/ITO, (B) WO_3/ITO, (C) WO_3/PDA/ITO, respectively and (D) the EDS spectrum of the Lys-WS_2/ITO, WO_3/ITO and WO_3/PDA/ITO. (E) Nyquist diagrams of (a) WO_3/ITO, (b) PDA-WO_3/ITO, (c) Ab/PDA-WO_3/ITO, (d) BSA/Ab/PDA-WO_3/ITO, (e) Ag/BSA/Ab/PDA-WO_3/ITO. (F) Photoresponses of (a) Lys-WS_2/ITO, (b) WO_3/ITO, (c) PDA-WO_3/ITO, (d) Ab/PDA-WO_3/ITO, (e) BSA/Ab/PDA-WO_3/ITO, (f) Ag/BSA/Ab/PDA-WO_3/ITO.

electron transfer resistance (R_{et}), owing to the favorable conductivity of WO_3. After covering with PDA, the R_{et} reduced, suggesting PDA can promote the electron transfer, and further improve the conductivity of the modified electrode. With the subsequent assembly of CYFRA21-1Ag, BSA and CYFRA21-1, the R_{et} stepped up. This was attributed to the excellent biocompatibility of the PDA film which can be assembled with proteins efficiently (Lee et al., 2007; Liu et al., 2014). Because of the insulating effect and hindrance effect of the biomaterials, the protein molecules hindered the mass transport and electron transfer of the photoactive materials to the electrode surface (Qileng et al., 2018). The stepwise change of the R_{et} verified the successful assembly of the final immunosensor.

We further monitored the change of photocurrent responses during the assembly process. As illustrated in Fig. 1F, the photoresponse for WS_2/ITO was small under the exciting light of 365 nm. The response for WO_3, however, increased prominently, implying that the photoelectric property improved significantly after oxidation of WS_2 to WO_3. And the photocurrent maintained steady (RSD = 0.5%) even after 30 days storage at room temperature. As expected, the photocurrent increased even higher after covering PDA film. The results validated that PDA can be a sensitizer to enhance the PEC performance of semiconductors by improving the conductivity of the modified electrode, shortening the carrier diffusion distance, improving light harvesting efficiency and charge collection efficiency (Fan et al., 2017; Ryu et al., 2015; Wei et al., 2013). The photocurrent intensity declined after Ab anchoring and BSA blocking, due to the steric hindrances of the insulating proteins, which impeded the contact of AA with the electrode interface. One the other hand, the proteins could also hinder the effect of exciting light to the photoelectric active material on the surface of the electrode. The current change of the modified process was consistent with the EIS results, indicating that Ag/BSA/Ab/PDA-WO_3 composite film was successfully formed on electrode surface. Therefore, WO_3 based nanomaterial has been successfully employed as highly sensitive photoelectric active material for biosensing platform construction. Moreover, the PDA film can not only act as a sensitizer for WO_3, but also provided a favorable basic biocompatible framework for biomolecules immobilization, thus hold great potential for immunosensor fabrication.

3.3. The optimization of PEC detection conditions

To achieve the best performance, critical experiment parameters including working potential, concentrations of AA and pH values were optimized (Fig. 2). Firstly, we evaluated the performance of the PDA-WO_3/ITO electrode under the potential ranging from 0 to 0.7 V. The working potential was a key parameter in the detection system. We can figure from the results in Fig. 2A that the photocurrent increased with the potential and maximized at 0.4 V. As higher potential system will be more vulnerable to substrate disturbance, 0.3 V was chosen for further detection.

AA acted as the electron donor to capture the photo generated holes and reduce the photo-oxidized PDA-film. We measured the photocurrents under the condition of various AA concentrations (0–50 mM). As illustrated in Fig. 2B, the photocurrent intensity enhanced along with the AA concentration and reached the maximum at 5 mM. Higher concentrations, on the contrary, will result in signal reduction. In this PEC system, when the photo-generated electrons were injected into the WO_3 nanomaterial, the PDA film could be regenerated by obtaining electron form the electron donor of AA (Yang and Hu, 2017), as shown in Scheme 2. However, overmuch AA will cause the excess absorbance in solution, thus impacting the irradiation arrived at the electrode interface (Wang et al., 2009). Hence, 5 mM AA was selected in the subsequent measurement.

We also investigated the influence of pH. The current change rose along with pH from 3.5 up to 7.4 and then decreased as further elevation of the pH value (Fig. 2C). This can be ascribed to that acid or alkali conditions inhibited the bioactivity of biomolecules (Akhtar et al., 2018; Feng et al., 2018; Wang et al., 2018), and pH 7.4 was more similar to physiological condition. Better bioactivity of biomolecules could favor the formation of immunocomplex layer on the electrode, which resulted in increasing current response change. This is because the immunocomplex layer on the electrode surface not only acted as the electron communication blocking layer, but also acted as the light blocking layer. Thus, we chose pH 7.4 for further detection.

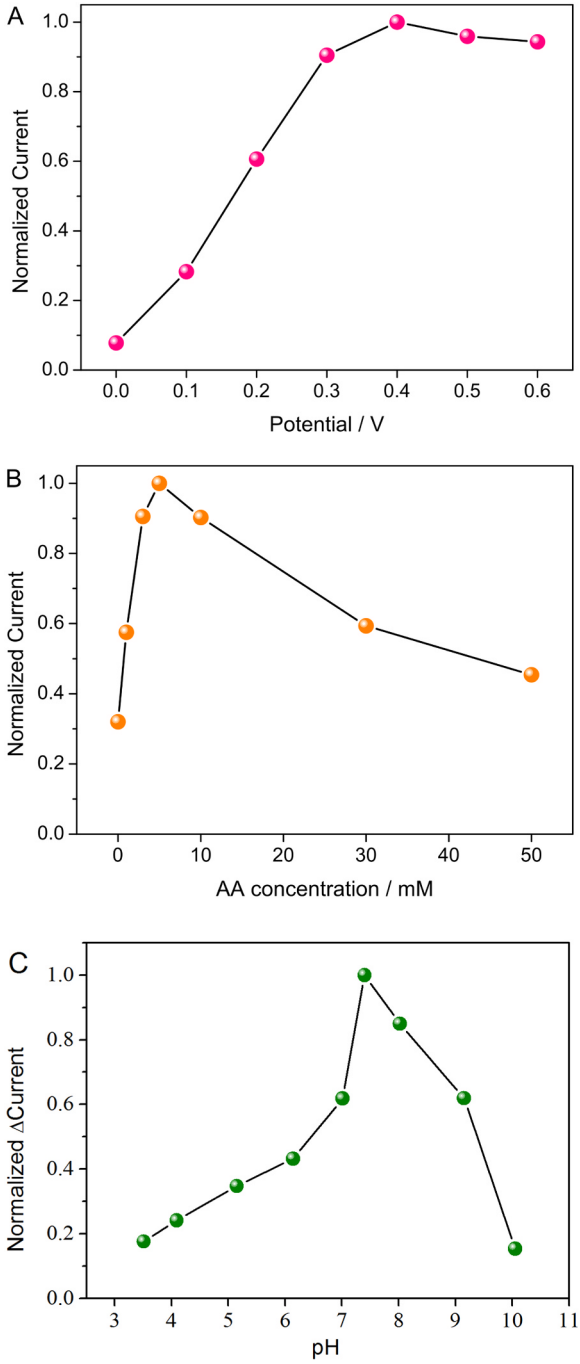

Fig. 2. Effects of the working potential, AA concentration and pH on the performance of the immunosensor.

3.4. Detection performance of the PDA/WO_3/ITO immunosensor

CYFRA21-1 was detected under the optimal condition (Fig. S1). The photocurrent for various concentrations of CYFRA21-1 was measured. And all the results were obtained from experiments repeated three

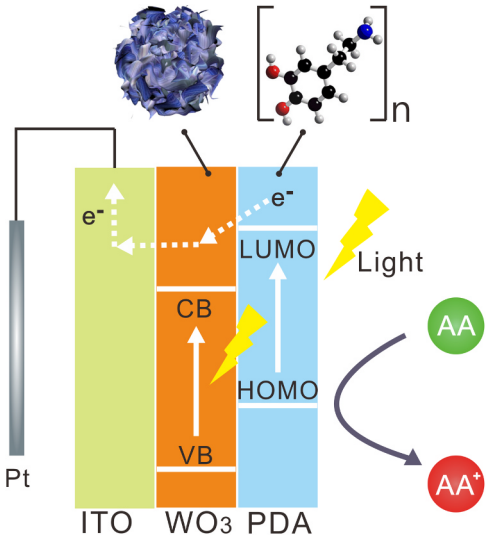

Scheme 2. Schematic illustration of the photocurrent generation mechanism.

times independently. It can be observed in Fig. 3A that the photocurrents decreased with increase of the CYFRA21-1 concentration. It can be understood that more CYFRA21-1molecules could bind to the immobilized antibodies, and the resulting antigen-antibody immunocomplex would lead to the decrease of the amperometric response. The proposed PEC immunosensor showed a linear response to CYFRA21-1concentration in the range of 10 pg mL^{-1}~100 ng mL^{-1}. The proposed immunosensor achieved a detection limit of 2.5 pg mL^{-1} for CYFRA21-1 (S/N = 3), which was significantly more sensitive than the commonly used electrochemical and fluorescent methods (Table 1) and recently reported PEC immunosensors (Table S1). Notably, our biosensing platform was facial to fabricate without any laborious procedures. The highly correlation between the concentration of CYFRA21-1 and the current intensity confirmed the proposed strategy that more target proteins will yield greater hindrance of the mass transport and electron transfer. It has been reported that the normal concentration of serum CYFRA21-1 was 0.1–3.3 ng mL^{-1} (Pujol et al., 2003). And the presented PDA/WO_3/ITO biosensor has met the requirement of sensitivity for real serum sample analysis, holding great promise for clinic application.

To further investigate the specificity of the PDA/WO_3 NCs based biosensor for CYFRA21-1, impact from interfering proteins was investigated, including CEA, FN, AFP and CA125. In Fig. 3B, the 2000-fold concentration of interfering protein (0.2 μg mL^{-1}) yielded much lower signals than the CYFRA21-1 (0.1 ng mL^{-1}), demonstrating the excellent specificity of our fabricated PEC sensor.

We also investigated the repeatability of the PDA-WO_3/ITO immunosensor by measuring the photocurrent of 100 pg mL^{-1} CYFRA21-1 for 6 times. And the relative standard deviation (RSD) was as low as 1.5%. After 30 days storage, the photocurrent response still remained 90%. Results above validated the outstanding repeatability and stability of the sensor.

3.5. Applications of the PDA/WO_3/ITO immunosensor

The robustness of our biosensing platforms was also verified with real biological samples. We determined the CYFRA21-1 in serum samples by standard addition methods. Different concentrations of CYFRA21-1 standard solution (2.00, 5.00, and 10.00 ng mL^{-1}) were added into serum samples and measured (Table S2). The recoveries were in the range of 98.4–103.5%, and the RSD were 4.45–7.22%. A *t*-test and an *F*-test performed at a 95% confidence level demonstrated that the results obtained by the proposed method and ELISA kit did not significantly differ (Table S3), indicating the PEC system was competent for clinical diagnosis application.

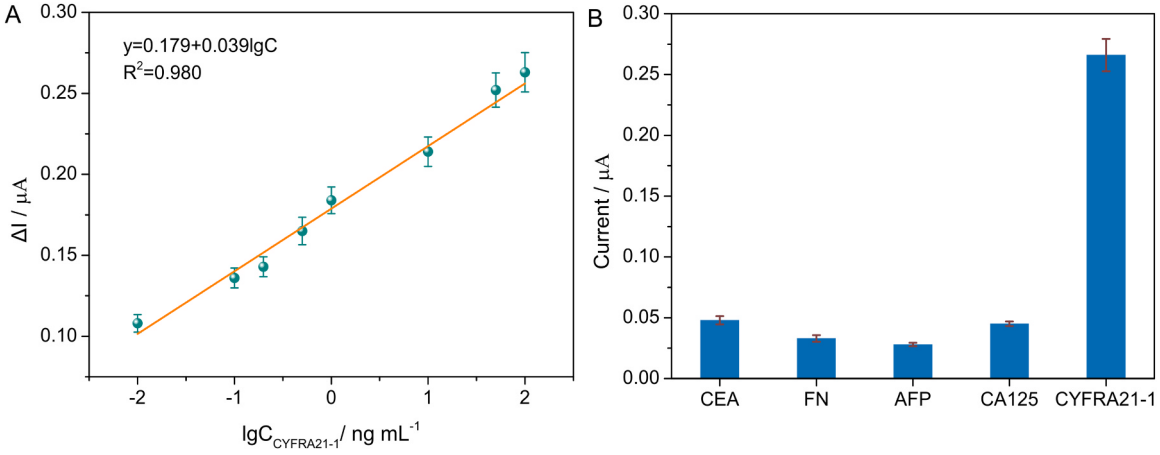

Fig. 3. PEC response (A) and linear regression curve (B) of different concentrations of CYFRA21-1 solutions. (C) PEC response to different kinds of proteins.

Table 1
Comparison between the proposed PEC sensor and other sensors for CYFRA 21–1 assay.

Detection method	Readout protocol	Dynamic range (ng mL^{-1})	Limit of detection (ng mL^{-1})	Reference
(APTES)/ZrO_2/ITO[a]	Electrochemistry	2–16	0.08	(Kumar et al., 2015)
Backscattering interferometry (BSI)	Fluorescence	0.156–10	0.23	(Olmsted et al., 2014)
APTES/ZrO_2–RGO/ITO[b]	Electrochemistry	2–22	0.122	(Kumar et al., 2016)
QPs-LFTS[c]	Fluorescence	1.3–480	0.16	(Chen et al., 2017)
PDA-WO_3/ITO	Photoelectrochemistry	0.01–100	0.0025	This work

[a] Aminopropyl triethoxy silane (APTES)/ Zirconia (ZrO_2)/ITO.
[b] Aminopropyl triethoxy silane (APTES)/Zirconia-reduced graphene oxide (ZrO_2–RGO)/ITO.
[c] Quantum dot-doped polystyrene nanoparticles-based lateral flow test strips.

4. Conclusions

In this work, by integration of the merits of WO_3 semiconductor nanomaterial and multifunctional PDA polymer, a novel biofunctional PDA/WO_3 NCs modified ITO hierarchical architecture was fabricated by simple thermal annealing and self-polymerization methods. The proposed PEC biosensor platform not only has preponderances in simple preparation, but also possesses excellent PEC activity, and can be used as good building blocks for biomolecule immobilization. The fabricated PEC sensor can be utilized for CYFRA 21-1 sensing with great sensitivity and broad dynamic range with four orders of magnitude. Owing to the great sensitivity and selectivity of the proposed platform, the PDA/WO_3 PEC sensor also performed well in complex serum matrixes. Notably, our work has promoted better understanding of the PEC properties of PDA/WO_3 NCs as well as shed novel light on the design and development of PEC biosensing platform. We foresee that the present work will contribute to addressing challenges in biomedical engineering by possessing great potential for application to other molecules ranging from cells, DNA to proteins.

Acknowledgments

We sincerely acknowledge the financial support of the National Natural Science Foundation of China (21675024, 21705082), Fujian Province Health Commission Young and Middle-Aged Talent Training Project (2018-ZQN-62), the Open Program for the Key Lab/Research Platform of the First Affiliated Hospital of Fujian Medical University (FYKFKT-201707), the Science and Technology Plan Projects of Nantong (MS120166023), the Natural Science Foundation of Jiangsu Province (BK20170444), the Joint Funds for the Innovation of Science and Technology, Fujian Province (2016Y9056, 2016Y9054).

Appendix A. Supporting information

Supplementary data associated with this article can be found in the online version at doi:10.1016/j.bios.2018.10.026.

References

Akhtar, M.H., Hussain, K.K., Gurudatt, N.G., Chandra, P., Shim, Y.B., 2018. Biosens. Bioelectron. 116, 108–115.
Ball, V., 2018. Catal. Today 301, 196–203.
Cai, J., Huang, J., Ge, M., Iocozzia, J., Lin, Z., Zhang, K.Q., Lai, Y., 2017. Small 13 (19).
Chen, Z.H., Liang, R.L., Guo, X.X., Liang, J.Y., Deng, Q.T., Li, M., An, T.X., Liu, T.C., Wu, Y.S., 2017. Biosens. Bioelectron. 91, 60–65.
Dong, Y.X., Cao, J.T., Liu, Y.M., Ma, S.H., 2017. Biosens. Bioelectron. 91, 246–252.
Fan, D., Wang, H., Khan, M.S., Bao, C., Wang, H., Wu, D., Wei, Q., Du, B., 2017. Biosens. Bioelectron. 97, 253–259.
Feng, J., Li, Y., Gao, Z., Lv, H., Zhang, X., Dong, Y., Wang, P., Fan, D., Wei, Q., 2018. Sens. Actuator B-Chem. 270, 104–111.
Grunnet, M., Sorensen, J.B., 2012. Lung Cancer 76 (2), 138–143.
Han, Q., Wang, R., Xing, B., Zhang, T., Khan, M.S., Wu, D., Wei, Q., 2018. Biosens. Bioelectron. 99, 493–499.
Kumar, S., Ashish, Kumar, S., Augustine, S., Yadav, S., Yadav, B.K., Chauhan, R.P., Dewan, A.K., Malhotra, B.D., 2018. Biosens. Bioelectron. 102, 247–255.
Kumar, S., Kumar, S., Tiwari, S., Srivastava, S., Srivastava, M., Yadav, B.K., Kumar, S., Tran, T.T., Dewan, A.K., Mulchandani, A., Sharma, J.G., Maji, S., Malhotra, B.D., 2015. Adv. Sci. 2 (8), 1500048.
Kumar, S., Sharma, J.G., Maji, S., Malhotra, B.D., 2016. Biosens. Bioelectron. 78, 497–504.
Kumar, S.G., Rao, K.S.R.K., 2015. Appl. Surf. Sci. 355, 939–958.
Lee, H., Dellatore, S.M., Miller, W.M., Messersmith, P.B., 2007. Science 318 (5849), 426–430.
Liu, B., Li, Y., Wan, H., Wang, L., Xu, W., Zhu, S., Liang, Y., Zhang, B., Lou, J., Dai, H., Qian, K., 2016. Adv. Funct. Mater. 26 (44), 7994–8002.
Liu, Y., Ai, K., Lu, L., 2014. Chem. Rev. 114 (9), 5057–5115.
Lu, N., Gao, A., Dai, P., Mao, H., Zuo, X., Fan, C., Wang, Y., Li, T., 2015. Anal. Chem. 87 (22), 11203–11208.
Mandal, D., Routh, P., Nandi, A.K., 2018. Small 14 (4).
Olmsted, I.R., Hassanein, M., Kussrow, A., Hoeksema, M., Li, M., Massion, P.P., Bornhop, D.J., 2014. Anal. Chem. 86 (15), 7566–7574.
Peng, H., Lin, D., Liu, P., Wu, Y., Li, S., Lei, Y., Chen, W., Chen, Y., Lin, X., Xia, X., Liu, A., 2017. Anal. Chim. Acta 992, 128–134.
Peng, H., Liu, P., Lin, D., Deng, Y., Lei, Y., Chen, W., Chen, Y., Lin, X., Xia, X., Liu, A., 2016. Chem. Commun. 52 (61), 9534–9537.
Pujol, J.L., Quantin, X., Jacot, W., Boher, J.M., Grenier, J., Lamy, P.J., 2003. Lung Cancer 39 (2), 131–138.
Qileng, A., Wei, J., Lu, N., Liu, W., Cai, Y., Chen, M., Lei, H., Liu, Y., 2018. Biosens. Bioelectron. 106, 219–226.
Qu, K., Zheng, Y., Jiao, Y., Zhang, X., Dai, S., Qiao, S.-Z., 2017. Adv. Energy Mater. 7 (9).
Ryu, G.M., Lee, M., Choi, D.S., Park, C.B., 2015. J. Mater. Chem. B 3 (22), 4483–4486.
Soria, J.C., Tan, D.S.W., Chiari, R., Wu, Y.L., Paz-Ares, L., Wolf, J., Geater, S.L., Orlov, S., Cortinovis, D., Yu, C.J., Hochmair, M., Cortot, A.B., Tsai, C.M., Moro-Sibilot, D., Campelo, R.G., McCulloch, T., Sen, P., Dugan, M., Pantano, S., Branle, F., Massacesi, C., de Castro Jr., G., 2017. Lancet 389 (10072), 917–929.
Tan, Y., Li, M., Ye, X., Wang, Z., Wang, Y., Li, C., 2018. Sens. Actuators B-Chem. 262, 982–990.
Wang, G.L., Yu, P.P., Xu, J.J., Chen, H.Y., 2009. J. Mater. Chem. C 113 (25), 11142–11148.
Wang, R., Ma, H., Zhang, Y., Wang, Q., Yang, Z., Du, B., Wu, D., Wei, Q., 2017a. Biosens. Bioelectron. 96, 345–350.
Wang, X., Gao, P., Yan, T., Li, R., Xu, R., Zhang, Y., Du, B., Wei, Q., 2018. Sens. Actuator B-Chem. 258, 1–9.
Wang, X., Xu, R., Sun, X., Wang, Y., Ren, X., Du, B., Wu, D., Wei, Q., 2017b. Biosens. Bioelectron. 96, 239–245.
Wang, Y., Gao, C., Ge, S., Yu, J., Yan, M., 2016. Biosens. Bioelectron. 85, 205–211.
Wei, Y., Kong, J., Yang, L., Ke, L., Tan, H.R., Liu, H., Huang, Y., Sun, X.W., Lu, X., Du, H., 2013. J. Mater. Chem. A 1 (16), 5045–5052.
Whaley, S.R., English, D.S., Hu, E.L., Barbara, P.F., Belcher, A.M., 2000. Nature 405 (6787), 665–668.
Yang, Q., Hao, Q., Lei, J., Ju, H., 2018. Anal. Chem. 90 (6), 3703–3707.
Yang, Y., Hu, W., 2017. Talanta 166, 141–147.
Zang, Y., Lei, J., Ju, H., 2017. Biosens. Bioelectron. 96, 8–16.
Zhang, J., Liu, Z., Liu, Z., 2016. ACS Appl. Mater. Interfaces 8 (15), 9684–9691.
Zhang, N., Zhang, L., Ruan, Y.F., Zhao, W.W., Xu, J.J., Chen, H.Y., 2017. Biosens. Bioelectron. 94, 207–218.
Zhao, W.W., Xu, J.J., Chen, H.Y., 2015. Chem. Soc. Rev. 44 (3), 729–741.
Zhao, W.W., Xu, J.J., Chen, H.Y., 2017. Biosens. Bioelectron. 92, 294–304.
Zhao, W.W., Xu, J.J., Chen, H.Y., 2018. Anal. Chem. 90 (1), 615–627.